

Resonant Frequencies of TE_{0mn} modes in multilayered dielectric-ferrite resonators with complex shapes

Krzysztof Derzakowski

Abstract—The method of evaluating the resonant frequencies of multilayered resonator containing demagnetized ferrites is presented. The detailed solution of Maxwell's equations for such a structure by means of the radial modes matching method for TE_{0mn} modes is given. The results of calculations using developed and launched computer program are given. Results of calculations are compared with those obtained by other method using CST simulator. These results are in close agreement, which proves the correctness of the method. The developed solution, and the software program can be used to measure the initial permeability of ferrites.

Keywords—dielectric resonator; Maxwell's equations; radial modes matching method; initial permeability

I. INTRODUCTION

THE development of materials technology makes that newly created materials have previously unattainable electrical and magnetic properties. They are very quickly adapted to the fabrication and construction of systems in the field of electronics. Materials produced and used in electronics have a wide range of relative permittivity and permeability. These parameters may vary depending on the frequency as well as a function of the direction (anisotropic dielectric, ferrites) and the applied external electric and magnetic field (ferroelectrics, ferrites). The use of such materials in electronics enforces the need for accurate knowledge of their electrical and magnetic parameters. It is therefore necessary to develop newer and better methods to measure these materials.

At microwave frequencies, for dielectric with a relative permittivity greater than 10, resonant methods are most often used, in particular dielectric resonator method [1]. The advantage of this method is very good accuracy to determine material parameters, as well as measurements are easy. The resonant frequency and the Q-factor of structure, which includes sample test material are measured at once [2]. The material parameters are determined from the equations describing the resonance conditions of the test structure. There are many ways to derive these equations, however, most accurate appear to be mode matching methods, either radial or axial.

There are numerous of studies to enable the calculation of the resonant frequency of the structure used in the measurement, but most commonly they involve simple structure composed of a

small number of layers of material [3]-[6]. The most advanced solution relates to a multilayer dielectric resonator which can contain up to 10 regions and 10 layers in each of them, but dielectrics included in the system are described by scalar relative permittivity [7]. In [8] you can find a solution for a structure consisting of 20 regions and 20 layers of dielectrics in each of them determined by tensor electric permittivity. The structure containing ferrite materials was analyzed in [9] and was composed of three regions and 10 layers in each.

You can use any electromagnetic simulator, e.g. CST [10], HFSS [11], QuickWave [12], to calculate the resonance frequency of a complex structure. However, each of these simulators use approximations of partial differential equations, so the accuracy of the calculations is limited. In the 3D simulators the structure is meshed and accuracy of the computations depends on the mesh size. Thus the accuracy depends on the quantization of space. It can also depend on the quantization of time (in FDTD), dispersion, round-off errors etc. The computation time in some simulators may be much longer than in the presented solution. The price of commercial electromagnetic simulators is also an important factor but it must be added that the 3D electromagnetic simulators can be used to any type of structures, which is their main advantage.

In this paper, a solution employing the radial modes matching method for the multilayered resonator containing dielectric and magnetic materials (ferrites), is presented. Although studies on the structure containing ferrites are presented in the literature, they are related to simple structures [3], [9]. In this work, a solution of the Maxwell equations for the multilayered resonator, which may contain up to 40 regions and 40 layers of each of them, which is more than exhaustive demand is presented.

The simplified general structure of the multilayered dielectric-ferrite resonator is shown in Fig. 1.

It consists of three regions I, II and III with axial symmetry. The amount of these regions can be equal to a maximum of 40 in the developed program. The first region thus has a cylindrical shape, the next ones are rings. In each region there is a number of layers of material having different relative complex permittivity and permeability. The structure is enclosed by a metal cylinder whose radius R_3 may be infinite. The structure does not affect constant or slowly varying external magnetic field. In this case, the magnetic properties of ferrites can be described by the initial permeability in the form of a scalar.

Krzysztof Derzakowski is with Institute of Radioelectronics and Multimedia Technology, Warsaw University of Technology, Poland (e-mail: Krzysztof.Derzakowski@pw.edu.pl).



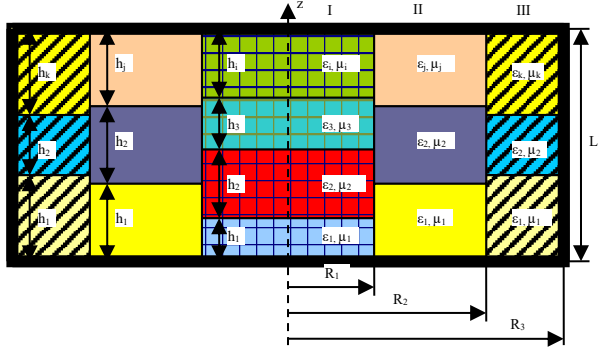


Fig. 1. The multilayered dielectric-ferrite resonator

II. THE SOLUTION OF BOUNDARY VALUE PROBLEM FOR THE RESONATOR WITH MAGNETIC MEDIA

Stated problem boils down to solve Maxwell's equations for such a structure. Due to the rotational symmetry of the analyzed structure the Maxwell equations will be solved in a cylindrical coordinate system.

Maxwell's equations in each layer of each region can be written as (given the absence of charges and currents sources):

$$\begin{cases} \nabla \times \vec{E} = j\omega \vec{B} & (1) \\ \nabla \times \vec{H} = j\omega \vec{D} & (2) \\ \nabla \cdot \vec{D} = 0 & (3) \\ \nabla \cdot \vec{B} = 0 & (4) \end{cases}$$

Taking into account the linearity and isotropy of the media belonging to the resonator the following are obtained:

$$\begin{cases} \nabla \times \vec{E} = j\omega \mu \vec{H} & (5) \\ \nabla \times \vec{H} = j\omega \epsilon \vec{E} & (6) \\ \nabla \cdot \vec{E} = 0 & (7) \\ \nabla \cdot \vec{H} = 0 & (8) \end{cases}$$

where: $\mu = \mu_d \mu_0$, and μ_d is a permeability for magnetic field equal to zero.

For TE_{0mn} modes, the electric field \vec{E} and magnetic field \vec{H} vectors take the following form: $\vec{E} = [0, 0, E_\varphi]$, $\vec{H} = [H_r, H_z, 0]$. It was also assumed that the non-zero components of these vectors are independent of the angle φ .

Now, we transform (5) using vector calculus and taking into account material properties we obtain (9):

$$\frac{i_z}{r} \frac{\partial}{\partial r} [r E_\varphi] - \frac{i_z}{r} \frac{\partial E_r}{\partial \varphi} + i_\varphi \frac{\partial E_r}{\partial z} - i_\varphi \frac{\partial E_z}{\partial r} + \frac{i_r}{r} \frac{\partial E_z}{\partial \varphi} - \frac{i_r}{r} \frac{\partial}{\partial z} [r E_\varphi] = -j\omega \mu [i_z H_z + i_\varphi H_\varphi + i_r H_r] \quad (9)$$

and taking into account the form of vectors \vec{E} and \vec{H} we obtain (10):

$$\frac{i_z}{r} \frac{\partial}{\partial r} [r E_\varphi] - \frac{i_r}{r} \frac{\partial}{\partial z} [r E_\varphi] = -j\omega \mu [i_z H_z + i_r H_r] \quad (10)$$

And finally, two independent equations (11, 12):

$$\begin{cases} \frac{1}{r} \frac{\partial}{\partial r} [r E_\varphi] = -j\omega \mu H_z & (11) \\ \frac{\partial E_\varphi}{\partial z} = j\omega \mu H_r & (12) \end{cases}$$

The same applies to (6).

$$\begin{aligned} \frac{i_z}{r} \frac{\partial}{\partial r} [r H_\varphi] - \frac{i_z}{r} \frac{\partial H_r}{\partial \varphi} + i_\varphi \frac{\partial H_r}{\partial z} - i_\varphi \frac{\partial H_z}{\partial r} + \frac{i_r}{r} \frac{\partial H_z}{\partial \varphi} + \\ - \frac{i_r}{r} \frac{\partial}{\partial z} [r H_\varphi] = -j\omega \epsilon [i_z E_z + i_\varphi E_\varphi + i_r E_r] \end{aligned} \quad (13)$$

and, finally we obtain (14)

$$\frac{\partial H_r}{\partial z} - \frac{\partial H_z}{\partial r} = j\omega \epsilon E_\varphi \quad (14)$$

Together with (11) and (12), the system of equations (15-17) is obtained.

$$\begin{cases} \frac{\partial H_r}{\partial z} - \frac{\partial H_z}{\partial r} = j\omega \epsilon E_\varphi & (15) \end{cases}$$

$$\begin{cases} \frac{1}{r} \frac{\partial}{\partial r} [r E_\varphi] = -j\omega \mu H_z & (16) \end{cases}$$

$$\begin{cases} \frac{\partial E_\varphi}{\partial z} = j\omega \mu H_r & (17) \end{cases}$$

Equations (15-17) describe the electromagnetic field in each layer with constant values ϵ and μ , and taking into account changes ϵ and μ in the "z" function will be made later.

From (16), $H_z = -\frac{1}{j\omega \mu r} \frac{\partial}{\partial r} (r E_\varphi)$ is calculated, and from (17),

$H_r = \frac{1}{j\omega \mu} \frac{\partial E_\varphi}{\partial z}$ is calculated and substituted into 15.

After, we obtain (18).

$$\frac{\partial^2 E_\varphi}{\partial z^2} + \frac{\partial}{\partial r} \left[\frac{1}{r} \frac{\partial}{\partial r} (r E_\varphi) \right] + k_0^2 \epsilon_r \mu_r E_\varphi = 0 \quad (18)$$

where: $k_0 = \omega_0 \sqrt{\epsilon_0 \mu_0} = \frac{2\pi}{\lambda_0}$.

The equation (18) is solved separately in each layer of each of the region by using the method of separation of variables, and then the solutions are "stitched" on the borders of regions ($r = R_1, R_2, R_3, \dots$), ensuring continuity of tangential components.

Assuming that in (18) $E_\varphi(r, z) = U(r) * \Phi(z)$, a system of two equations of a single variable is obtained:

$$\begin{cases} \frac{d^2 \Phi(z)}{dz^2} + [k_0^2 \epsilon_r \mu_r - \lambda_m] \Phi(z) = 0 & (19) \end{cases}$$

$$\begin{cases} r^2 \frac{d^2 U(r)}{dr^2} + r \frac{dU(r)}{dr} + (\lambda_m r^2 - 1) U(r) = 0 & (20) \end{cases}$$

where: $k_0^2 = \omega^2 \epsilon_0 \mu_0$, ϵ_r - relative permittivity and μ_d - relative initial permeability.

Equation (20) is the first-order Bessel equation for $\lambda_m > 0$, and the first-order modified Bessel equation for $\lambda_m < 0$. Its solutions for $\lambda_m > 0$ are Bessel functions of the first kind - $J_1(\sqrt{\lambda_m} r)$ and Neuman functions (Bessel functions of the second kind) - $N_1(\sqrt{\lambda_m} r)$. And for $\lambda_m < 0$. solutions of (20) are modified Bessel functions of the first kind - $I_1(\sqrt{\lambda_m} r)$ and the second kind - $K_1(\sqrt{\lambda_m} r)$. It should be noticed that for the I-st region taking into account the Neuman function is not justified physically.

In each layer of a given region, the permittivity and permeability are constant and equal to ϵ_{r_i} and μ_{r_i} , respectively, and the solutions of (19) are the functions $\Phi_m(z)$ which are a linear combination of trigonometric functions of the type $\sin(v_{m_i}z)$ and $\cos(v_{m_i}z)$. Where: $v_{m_i}^2 = k_0^2 \epsilon_{r_i} \mu_{r_i} - \lambda_m$:

If $v_{m_i}^2 < 0$, the trigonometric functions should be replaced with appropriate hyperbolic functions, i.e. $\sinh(v_{m_i}z)$ and $\cosh(v_{m_i}z)$.

Since the $\Phi_m(z)$ functions must be defined over the entire height of a given region, appropriate continuity conditions must be ensured on the electrical walls and on the separation planes of individual layers. These conditions are identical to the conditions for the E_φ component of the electromagnetic field.

The E_φ and H_z field components in each region are a linear combination of waveguide modes, so the relationships for the electromagnetic field components can be written (assuming that the radius of the third area extends to infinity):

$$E_\varphi^I(r, z) = \sum_{i=0}^{\infty} \frac{a_m}{\sqrt{\lambda_m^I}} J_1\left(\sqrt{\lambda_m^I} r\right) \Phi_m^I(z) \quad (21)$$

$$E_\varphi^{II}(r, z) = \sum_{i=0}^{\infty} \left[\frac{b_m}{\sqrt{\lambda_m^{II}}} J_1\left(\sqrt{\lambda_m^{II}} r\right) + \frac{c_m}{\sqrt{\lambda_m^{II}}} N_1\left(\sqrt{\lambda_m^{II}} r\right) \right] \Phi_m^{II}(z) \quad (22)$$

$$E_\varphi^{III}(r, z) = \sum_{i=0}^{\infty} \frac{d_m}{\sqrt{\lambda_m^{III}}} K_1\left(\sqrt{\lambda_m^{III}} r\right) \Phi_m^{III}(z) \quad (23)$$

$$H_z^I(r, z) = \frac{j}{\omega \mu_0 \mu_r^I} \sum_{i=0}^{\infty} a_m J_0\left(\sqrt{\lambda_m^I} r\right) \Phi_m^I(z) \quad (24)$$

$$H_z^{II}(r, z) = \frac{j}{\omega \mu_0 \mu_r^{II}} \sum_{i=0}^{\infty} \left[b_m J_0\left(\sqrt{\lambda_m^{II}} r\right) + c_m N_0\left(\sqrt{\lambda_m^{II}} r\right) \right] \Phi_m^{II}(z) \quad (25)$$

$$H_z^{III}(r, z) = \frac{j}{\omega \mu_0 \mu_r^{III}} \sum_{i=0}^{\infty} \frac{d_m}{\sqrt{\lambda_m^{III}}} K_0\left(\sqrt{\lambda_m^{III}} r\right) \Phi_m^{III}(z) \quad (26)$$

where: a_m , b_m , c_m and d_m are complex constants,

Due to the negligibly small values of the higher components of the series, the summation can be limited to a finite number of elements N . The coefficients a_m , b_m , c_m and d_m should be selected to ensure the continuity of the electromagnetic field at the boundaries of the regions, i.e. to:

$$H_z^I(R_1, z) - H_z^{II}(R_1, z) = 0 \quad (27)$$

$$E_\varphi^I(R_1, z) - E_\varphi^{II}(R_1, z) = 0 \quad (28)$$

$$H_z^{II}(R_2, z) - H_z^{III}(R_2, z) = 0 \quad (29)$$

$$E_\varphi^{II}(R_2, z) - E_\varphi^{III}(R_2, z) = 0 \quad (30)$$

In the case of a finite number of terms fulfilling the conditions of equality is impossible for all z . Therefore, these coefficients are determined from the condition that the mean square error

(functional) component of the difference on either side of the boundary reached the minimum value. The corresponding functionals have the form (here written for the three regions):

$$F_1 = \int_S |H_z^I(R_1, z) - H_z^{II}(R_1, z)|^2 ds \quad (31)$$

$$F_2 = \int_S |E_\varphi^I(R_1, z) - E_\varphi^{II}(R_1, z)|^2 ds \quad (32)$$

$$F_3 = \int_S |H_z^{II}(R_2, z) - H_z^{III}(R_2, z)|^2 ds \quad (33)$$

$$F_4 = \int_S |E_\varphi^{II}(R_2, z) - E_\varphi^{III}(R_2, z)|^2 ds \quad (34)$$

Functionals achieve these minimum values if and only if their derivatives with respect to unknown coefficients are equal to zero (Rayleigh-Ritz method). After differentiating F_1 with respect to a_m , F_2 with respect to b_m , F_3 with respect to c_m and F_4 with respect to d_m , a system of $4N$ linear equations is obtained, allowing the determination of the unknown constants a_m , b_m , c_m and d_m (35).

$$\tilde{W} \begin{bmatrix} a_1 \\ a_2 \\ \dots \\ d_m \end{bmatrix} = 0 \quad (35)$$

This system has a non-zero solution if and only if its determinant is equal to zero

$$\det \tilde{W} = 0 \quad (36)$$

The matrix \tilde{W} with dimensions $4N \times 4N$, for three regions, has the form (37), and its elements are presented in Table I.

$$\tilde{W} = \begin{bmatrix} U_1 & U_2 & U_3 & U_4 \\ U_5 & U_6 & U_7 & U_8 \end{bmatrix} \quad (37)$$

where: U_4 and U_5 are matrices with zero elements, and the remaining matrices have the form of $U_i = [v_{i1} \ v_{i2}]^T$.

TABLE I
ELEMENTS OF W MATRIX FOR THREE REGIONS

i	$v_{qk}^{i1}(q, k = 1, 2, \dots, N)$	$v_{qk}^{i2}(q, k = 1, 2, \dots, N)$
1	$J_0(h_i^I R_1) \left\langle \frac{\Phi_k^I(z) \Phi_q^{I*}(z)}{\mu_r^I} \right\rangle$	$\frac{J_1(h_i^I R_1)}{h_i^I} \langle \Phi_k^I(z) \Phi_q^{I*}(z) \rangle$
2	$J_0(h_i^{II} R_1) \left\langle \frac{\Phi_k^{II}(z) \Phi_q^{II*}(z)}{\mu_r^{II}} \right\rangle$	$\frac{J_1(h_i^{II} R_1)}{h_i^{II}} \langle \Phi_k^{II}(z) \Phi_q^{II*}(z) \rangle$
3	$N_0(h_i^{II} R_1) \left\langle \frac{\Phi_k^{II}(z) \Phi_q^{II*}(z)}{\mu_r^{II}} \right\rangle$	$\frac{N_1(h_i^{II} R_1)}{h_i^{II}} \langle \Phi_k^{II}(z) \Phi_q^{II*}(z) \rangle$
6	$J_0(h_i^{II} R_2) \left\langle \frac{\Phi_k^{II}(z) \Phi_q^{II*}(z)}{\mu_r^{II}} \right\rangle$	$\frac{J_1(h_i^{II} R_2)}{h_i^{II}} \langle \Phi_k^{II}(z) \Phi_q^{II*}(z) \rangle$
7	$N_0(h_i^{II} R_2) \left\langle \frac{\Phi_k^{II}(z) \Phi_q^{II*}(z)}{\mu_r^{II}} \right\rangle$	$\frac{N_1(h_i^{II} R_2)}{h_i^{II}} \langle \Phi_k^{II}(z) \Phi_q^{II*}(z) \rangle$
8	$K_0(h_i^{III} R_2) \left\langle \frac{\Phi_k^{III}(z) \Phi_q^{III*}(z)}{\mu_r^{III}} \right\rangle$	$\frac{-K_1(h_i^{III} R_2)}{h_i^{III}} \langle \Phi_k^{III}(z) \Phi_q^{III*}(z) \rangle$

where: $\langle \Phi_k^{(\alpha)}(z) \Phi_q^{(\beta)}(z) \rangle = \int_0^{L'} \Phi_k^{(\alpha)}(z) \Phi_q^{(\beta)}(z) dz$, and $h_i^{(\alpha)} = \sqrt{\lambda_i^{(\alpha)}}$.

III. RESULTS AND DISCUSSION

This section presents the results of the calculations of the resonant frequency of the dielectric-ferrite resonator in the form of a cylinder and a sphere. The simulations started with determining the resonant frequencies of various TE_{0mn} modes for a cylindrical resonator placed in a metal cavity with a height equal to the height of the resonator and a radius much larger than the radius of the cylinder. The diameter of the cylinder was equal to its height and equal to 8.89 mm. The analyzed ferrite had a permittivity of 15.66, and the permeability was varied from 0.35 to 1 [3]. For such a structure, determining the resonance frequency is very simple and does not require advanced methods. The results of calculations are shown in Fig. 2. The calculated values of the resonant frequency for the first three TE_{0mn} modes as a function of initial permeability are shown.

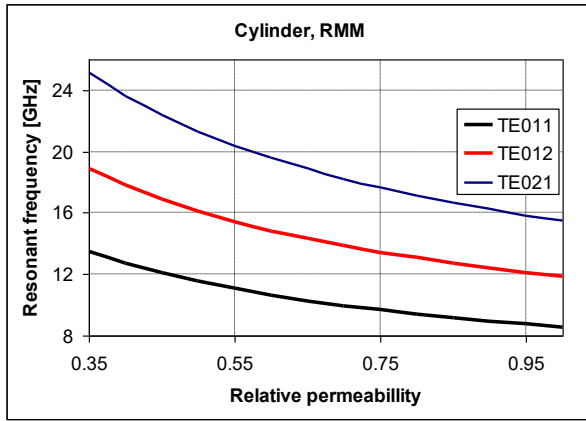


Fig. 2. Resonant frequency as a function of initial permeability obtain by means of radial modes matching

For comparison, Fig. 3 shows the results obtained using the CST electromagnetic simulator. As you can see, the results are almost identical, which is clear from Fig. 4, which shows the relative difference of calculations with both programs R_f . The relative difference of resonant frequencies was defined as (38):

$$R_f = \frac{f_{CST} - f_{RMM}}{f_{RMM}} \cdot 100 [\%] \quad (38)$$

where: R_f – the relative difference of frequencies, f_{RMM} – the resonant frequency obtained by means of the radial modes matching method, f_{CST} – the resonant frequency obtained by means of the CST electromagnetic simulator.

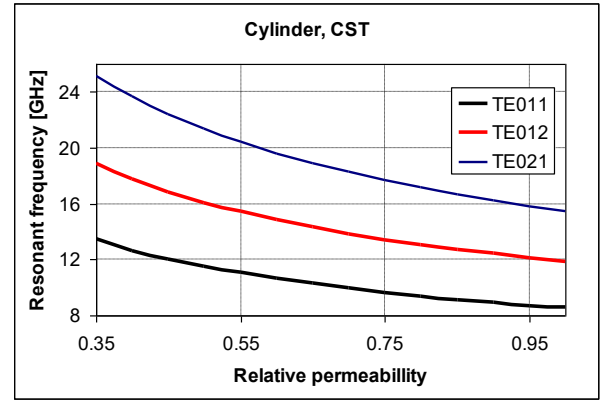


Fig. 3. Resonant frequency as a function of initial permeability by means of CST simulator

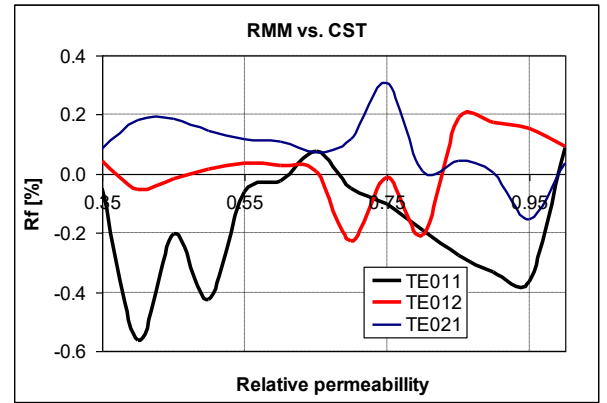


Fig. 4. The relative difference of resonant frequencies R_f as a function of initial permeability

As can be seen from Fig. 4, R_f ranges from -0.6 to 0.4 percent. This is a very good agreement of the obtained results, especially when taking into account the relationship between the resonant frequency calculated by the CST simulator and the place of resonator excitation.

The cylinder with a diameter equal to its height can be considered a very rough approximation of a sphere. In the radial modes matching method, a complex structure can be obtained by dividing it into regions and layers that are cylinders and rings. This division for a sphere is shown in Fig. 5.

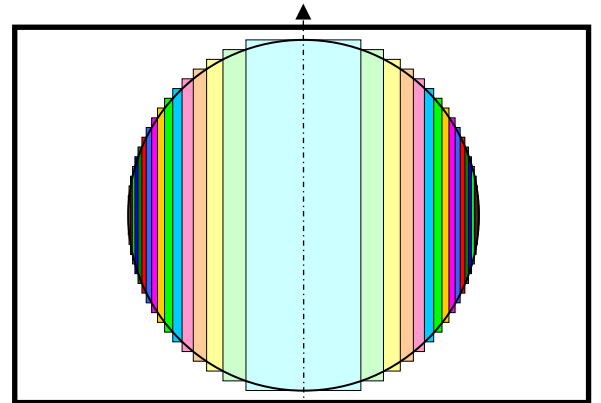


Fig. 5. The sphere divided in a radial modes matching method

To calculate the subsequent outer radii of the regions, proceed as follows:

- the diameter of the sphere R is divided into K equal sections with the value h_k ,
- the height of the next region h_i is calculated from the formula:

$$h_i = 2R - 2h_k(i - 1)$$

- the radius of the next region R_i is obtained from the formula:

$$R_i = \sqrt{R^2 - \left[R \left(\frac{K-1}{K} \right) \right]^2}$$

An example of the values of the heights and radii of the regions of the approximated sphere divided into 20 regions is presented in Table II.

TABLE II
AN APPROXIMATION OF A SPHERE IN PRESENTED METHOD

i	Radius [mm]	Height [mm]
1	1.387951	8.89
2	1.937531	8.4455
3	2.341549	8.001
4	2.667000	7.5565
5	2.940091	7.112
6	3.174365	6.6675
7	3.377908	6.223
8	3.556000	5.7785
9	3.712307	5.334
10	3.849483	4.8895
11	3.969512	4.445
12	4.073910	4.0005
13	4.163852	3.556
14	4.240260	3.1115
15	4.303853	2.667
16	4.355193	2.2225
17	4.394709	1.778
18	4.422719	1.3335
19	4.439440	0.889
20	4.445000	0.4445

The accuracy of mapping the sphere by such division depends on the number of regions. Therefore, calculations were carried out for various numbers of regions in order to determine the number of ones enabling a sufficient approximation of the sphere. The results of these calculations are presented in Fig. 6 and 7.

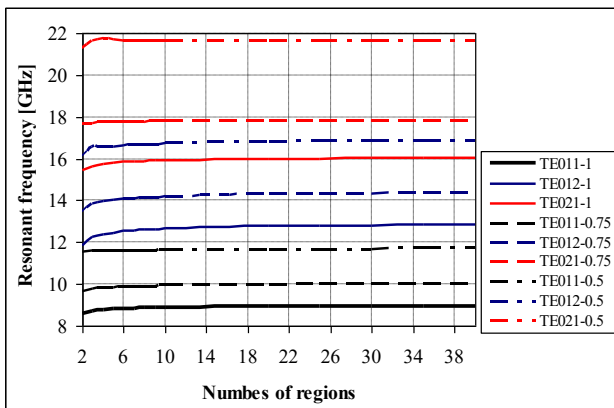


Fig. 6. Resonant frequencies of TE_{0mn} modes as a function of numbers of regions for different permeability (TE_{0mn}-1 - $\mu=1$, TE_{0mn}-0.75 - $\mu=0.75$, TE_{0mn}-0.5 - $\mu=0.5$)

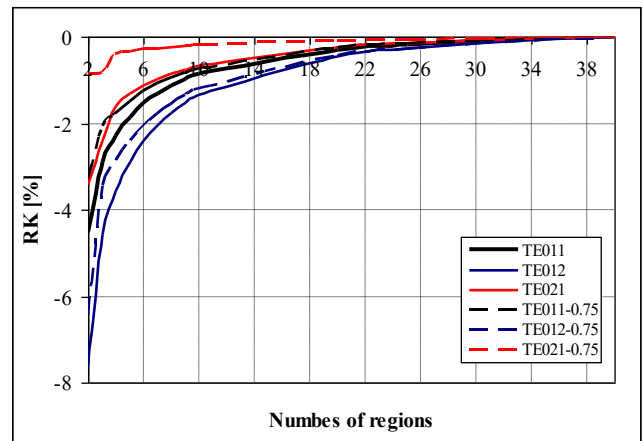


Fig. 7. Resonant frequencies of TE_{0mn} modes as a function of numbers of regions for different permeability (TE_{0mn}-1 - $\mu=1$, TE_{0mn}-0.75 - $\mu=0.75$, TE_{0mn}-0.5 - $\mu=0.5$)

R_k values defined as the relative difference in the resonant frequency for a specific value of the number of regions in relation to the maximum number of these regions (40) are described by the formula (39):

$$R_f = \frac{f_i - f_{max}}{f_{max}} \cdot 100 [\%] \quad (39)$$

where: R_f – the relative difference of frequencies, f_{max} – the resonant frequency obtained for maximum number of regions, f_i – the resonant frequency obtained for i regions.

As can be seen from Fig. 6, as the number of areas increases, the values of the calculated resonant frequencies stabilize towards the asymptotic value. This is clearly visible in Fig. 7, where for the number of regions above 30, changes in resonant frequencies do not exceed 0.2 percent.

Similarly to the cylinder, calculations were made for a sphere ($K = 30$) as a function of initial permeability for three TE_{0mn} modes. The results are presented in Fig. 8. Calculations were also made using the CST simulator. The results are presented in Fig. 9 along with calculations using the radial modes matching method.

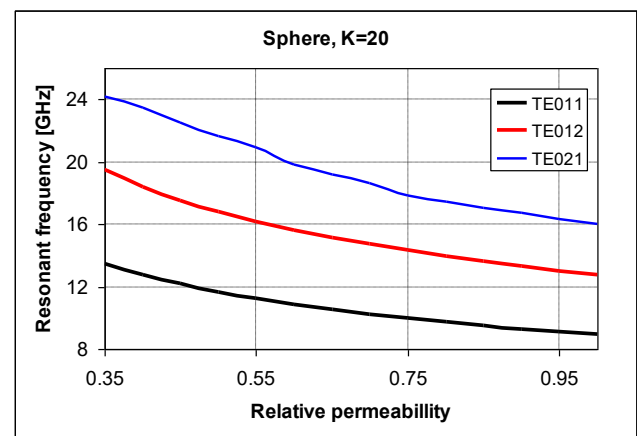


Fig. 8. Resonant frequency as a function of initial permeability obtain by means of radial modes matching.

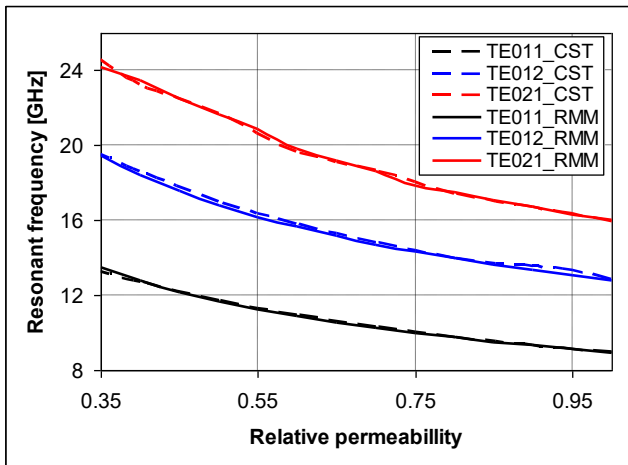


Fig. 9. Resonant frequency as a function of initial permeability obtain by means of radial modes matching and CST simulator.

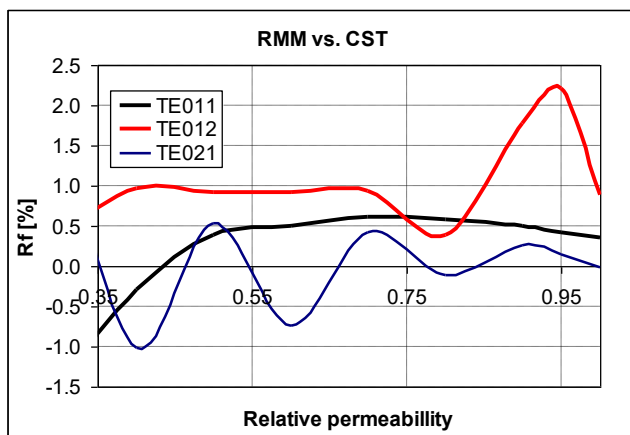


Fig. 10. The relative difference of resonant frequencies R_f as a function of initial permeability for analyzed sphere.

The differences in the resonant frequencies calculated by both methods are greater than for the cylinder, which is clearly visible in Fig. 10. This is probably due to not carefully selected excitation points in the CST simulator. It may also result from taking into account too few waveguide modes, which probably resulted in a not very smooth curve for the TE₀₂₁ mode (see Fig. 8).

CONCLUSION

The paper presents the application of the radial modes matching method to determine the resonant frequencies of TE_{0mn} species in a multilayer resonance structure containing dielectric and ferrite materials. The solution of Maxwell's

equations for TE_{0mn} modes is presented. A computer program was developed and launched enabling the analysis of structures composed of a maximum of 40 regions and 40 layers in each. This allows you to analyze complex structures such as a cone, a sphere, etc. The work deals with a sphere as an example structure. The results of calculations as a function of the initial permeability are presented, comparing them with the results obtained using the CST electromagnetic simulator. An analysis of the influence of the number of regions on the accuracy of calculations of resonant frequencies in the sphere was carried out. The obtained results allow the conclusion that the radial type matching method can be successfully used to analyze axisymmetric structures with complex shapes.

REFERENCES

- [1] J. Krupka, "Frequency domain complex permittivity measurements at microwave frequencies"; Measurement Science and Technology, vol.17, 2006, R55–R70. doi: 10.1088/0957-0233/17/6/R01
- [2] A. Abramowicz, J. Modelski, "Dielectric resonators and their applications"; PWN, 1990, (in Polish)
- [3] W. Courtney, "Analysis and evaluation of a method of measuring the complex permittivity and permeability of microwave insulators"; IEEE Trans. on Microwave Theory and Techniques, vol. 18, no. 8, pp. 476-485, Aug. 1970. doi:10.1109/TMTT.1970.1127271
- [4] S. Maj, J. Modelski, "Application of a dielectric resonator on microstrip line for measurement of complex permittivity"; in Proc. IEEE MTT International Microwave Symposium, San Francisco, 1984. doi:10.1109/MWSYM.1984.1131849
- [5] J. Krupka, "Resonant modes in shielded cylindrical ferrite and single-crystal dielectric resonators"; IEEE Trans. on Microwave Theory and Techniques, Vol. 37, No. 4, pp. 691-696, April 1989. doi:10.1109/22.18841
- [6] K. Derzakowski, A. Abramowicz, J. Krupka, "Whispering gallery resonator method for permittivity measurements", Journal on Telecommunications and Information Technology, No.1, pp.43-47, 2002.
- [7] S. Maj, "Metoda wyznaczania częstotliwości drgań własnych i jej zastosowanie do analizy wielowarstwowego cylindrycznego rezonatora dielektrycznego"; PhD Thesis, Warsaw, 1987
- [8] K. Derzakowski, "Full Wave Analysis of Multilayered Cylindrical Resonator Containing Uniaxial Anisotropic Media", Progress in Electromagnetics Research M, vol. 101, pp. 101-115, 2021. doi:10.2528/PIERM20120804
- [9] K. Derzakowski, "Complex resonant frequencies of multilayered ferrite resonator"; in Proc. Progress in Electromagnetics Research Symposium PIERS-94, Noordwijk, , pp.1253-1256, 1994
- [10] www.3ds.com - CST Studio - Electromagnetic field simulation software
- [11] www.ansys.com - 3D Electromagnetic Field Simulator for RF and Wireless
- [12] www.qwed.eu - Software for Electromagnetic Design
- [13] K. Derzakowski, "Full Wave Analysis of Multilayered Cylindrical Resonator Containing Uniaxial Anisotropic Media", Progress in Electromagnetics Research M, vol. 101, pp. 101-115, 2021. doi:10.2528/PIERM20120804